

## ■ Amyloid Fibers | Hot Paper |

## ● Supramolecular Regulation of Polydopamine Formation by Amyloid Fibers

J. H. Shin<sup>+</sup>,<sup>[a]</sup> Nghia T. K. Le<sup>+</sup>,<sup>[a]</sup> Hongje Jang,<sup>[b]</sup> Taehoon Lee,<sup>\*,[a]</sup> and Kyungtae Kang<sup>\*,[a]</sup>

**Abstract:** Polydopamine (PD) and melanin species are chemically complex systems, the formation and properties of which are incompletely understood. Inspired by the role of functional amyloids in melanin biosynthesis, this paper examines the influences of the supramolecular structure of amyloids on oxidative polymerization of dopamine. Kinetic analyses on the formation of PD species in the presence of hen egg white lysozyme (HEWL) fibers or soluble HEWL revealed that both forms gave rise to the total quantity of PD

species, but the rate of their formation could be accelerated only by the amyloid form. PD species formed with HEWL fibers showed a morphology of bundled fibers, whereas those with soluble HEWL had a mesh-like structure. Amyloid fibers of recombinant Pmel17 had properties similar to those of HEWL fibers in modulating PD formation. The results presented here suggest how nature designs functionality with an amyloid structure and can help understand and engineer chemistries of other functional amyloids.

## Introduction

Despite its short history, the development of polydopamine (PD)-based surface chemistry has impacted a vast range of materials fields such as biomedical, energy, optical materials, and others.<sup>[1]</sup> The formation of PD films is a material-independent, simple, and inexpensive method for chemical surface modification, with susceptibility to further functionalization with amine- or thiol-containing molecules. PD is formed by oxidative polymerization of dopamine under alkaline conditions, which is often initiated by simple dip-coating of samples. Although it is operationally simple, the exact molecular identities and chemical processes involved in the formation of PD remain poorly defined. It is now generally accepted that PD is noncovalent heterogeneous complex of oligomeric species derived from oxidation of dopamine, as strikingly similar to eumelanin in organisms.<sup>[2]</sup> In the case of eumelanin, L-dopa, instead of dopamine, is used as a major precursor and its oxidation is regulated tightly by enzymes. Studying eumelanin and other types of melanin (e.g., pheomelanin and neuromelanin) is a much older topic than PD, relatively oriented toward elucidating the origin



of its various properties (e.g., broad light absorption, thermal relaxation, radical properties, and anti-oxidant properties). Publications on PD were more centered on its potential to be interfaced with various applied fields. However, comprehensive approaches that combine knowledge and tools from the two fields are still rare except a few initiating efforts.<sup>[3]</sup> Melanin and PD are very similar in that they are complex systems originating from oxidation of catechols, but recent evidence suggests that apparent differences also exist, including detailed chemical composition, surface-coating properties, radical properties, and so on.

One interesting aspect (and a remarkable difference from PD formation) of melanin biosynthesis is the central role of functional amyloids, which are nontoxic but rather beneficial amyloid structures intentionally designed by organisms.<sup>[4]</sup> Pmel17, a type I transmembrane glycoprotein expressed in melanosomes of melanocytes and retinal pigment epithelium, is cleaved interluminally and forms amyloid fibers capable of templating and catalyzing the formation of melanin pigments inside melanosomes. The intraluminal region of Pmel17 is composed of multiple subdomains, such as N-terminal domain (NTD), polycystic kidney disease domain (PKD), and repeat domain (RPT), each of which exhibits amyloidogenic properties with different propensities when expressed *in vitro*.<sup>[5]</sup> During the maturation of a melanosome, Pmel17 undergoes multiple processes of cleavage and glycosylation, before forming amyloid fibers. The exact role of Pmel17 fiber is still unclear, except that it is indispensable in melanogenesis; one currently accepted hypothesis is that it sequesters potentially toxic intermediates generated during melanin synthesis by confining them within itself. However, the chemical origin of such amyloid-based regulation of melanin biosynthesis remains undressed.

[a] J. H. Shin,<sup>+</sup> N. T. K. Le,<sup>+</sup> Dr. T. Lee, Prof. Dr. K. Kang  
Department of Applied Chemistry  
Kyung Hee University, 1732 Deogyong-daero  
Yongin, Gyeonggi 17104 (Republic of Korea)  
E-mail: thlee@khu.ac.kr  
kkang@khu.ac.kr

[b] Prof. Dr. H. Jang  
Department of Chemistry, Kwangwoon University  
20 Gwangwoon-ro, Nowon-gu, Seoul 01897 (Republic of Korea)

[\*] These authors contributed equally to this work.

 Supporting information and the ORCID identification number(s) for the author(s) of this article can be found under:  
 <https://doi.org/10.1002/chem.202000437>.

Independent of the context of melanin biosynthesis, catechol derivatives (e.g., dopamine, epinephrine, epigallocatechin-3-gallate (EGCG), and flavonoids) have been frequently illuminated in studies dealing with pathological amyloids,<sup>[6]</sup> since they were shown to perturb the formation of amyloids and even, in some cases, disassemble preformed ones. For example, dopamine and L-dopa have been suggested to disassemble fibers of amyloid- $\beta$  (A $\beta$ ) or other proteins.<sup>[7]</sup> EGCG, a major component of green tea extract<sup>[8]</sup> and flavonoids,<sup>[9]</sup> was repeatedly shown to remodel amyloid aggregation of A $\beta$  proteins toward less toxic species. In case of Parkinson's disease, in which pathological amyloids appear primarily in dopaminergic neurons, dopamine could modulate the conformation and toxicity of amyloids made of  $\alpha$ -synuclein.<sup>[10]</sup> Although not proved unambiguously, evidence suggests that the oxidative polymerization of catechol-bearing molecules, or intermediates formed therein, is responsible for their observed influence on the amyloid structures.

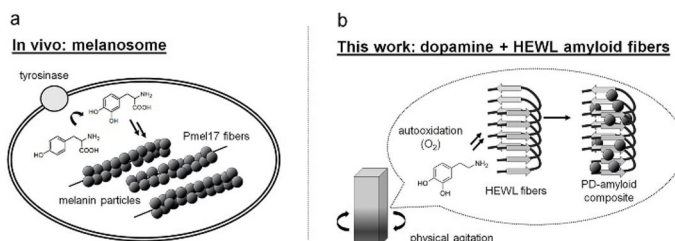
As shown above, many scattered clues found from studies of Pmel17 in melanin biosynthesis to those of pathological amyloids, suggest the existence of multifaceted interactions between catechol groups and amyloidogenic proteins, with their molecular-level details mostly veiled. This is primarily because of the complex nature of the chemistries related to the both species (catechols and amyloids) and the lack of analytical tools for precisely identifying multiple intermediate species formed by their interactions. So far, experimental conclusions that are agreed widely are as follows: (i) the influences are mutual. Catechols influence the formation of amyloids, and amyloid fibers influence the process of oxidative polymerization of catechols.<sup>[11]</sup> (ii) Catechols tend to bind (covalently or noncovalently) to amyloids.<sup>[12]</sup> (iii) Interacting with catechols makes amyloids invisible to amyloid-specific dyes (Thioflavin T (ThT) and Congo Red) and the resultant molecular complexes (if any) generally loses cytotoxicity.<sup>[13]</sup> (iv) The above characteristics are observed consistently for amyloids made of different proteins interacting with catechols, implying that it may be the supramolecular structure (or morphology) rather than a particular functional group or a sequence that interacts with catechols.

To date, chemical approaches have been primarily pursued to seek catechols that can suppress pathological amyloids; few studies have focused on the oxidative polymerization of catechols being regulated by amyloid supramolecular structures. This work specifically aims to examine influences of amyloid fibers on the process of PD formation and its final properties. We started with the following questions: (i) How do general amyloid fibers influence the kinetics and efficiency of PD formation? (ii) Would amyloid fibers formed from biologically irrelevant proteins affect PD formation similar to how Pmel17 affects melanin biosynthesis? (iii) How do the PD-amyloid composites differ from those formed spontaneously without fibers?

## Results and Discussion

### Experimental design

Theoretically, amyloids can be generated from any kind of folded proteins upon a proper denaturing treatment unique for each protein.<sup>[14]</sup> Hen egg white lysozyme (HEWL) has been extensively used to generate amyloid fibers with multiple developed experimental protocols,<sup>[15]</sup> since HEWL is easily available, but still shows high sequence homology with human lysozyme, which is pathologically responsible for hereditary systematic amyloidosis. We chose HEWL based on the assumption that it is the supramolecular structure of amyloids, rather than their specific sequence, that is capable of interacting with catechols. A previous work showed that amyloid fibers made of other pathological proteins irrelevant to melanin biosynthesis (A $\beta$  and  $\alpha$ -synuclein) could also facilitate the formation of melanin-like species.<sup>[4]</sup> We generated amyloid fibers of HEWL by denaturing HEWL with a high concentration of guanidine hydrochloride (GdnHCl),<sup>[16]</sup> and used them to template/accelerate the spontaneous oxidative polymerization of dopamine. We used dopamine, instead of more biologically relevant L-dopa, because their oxidative polymerizations are chemically similar, and previous studies focused more on PD formation. The pH of the reaction mixture was set to 7.4 without other oxidants, in which the spontaneous formation of PD occurs much slowly, enabling more detailed investigation on the kinetics of PD formation, and on the initial structures formed at the surface of the fibers (Scheme 1).



**Scheme 1.** a) Schematic of melanin synthesis in a melanosome (in vivo). b) Schematic of amyloid-templated PD formation. To observe the polymerization process in more detail, experimental conditions were set to neutral pH with constant physical agitation.

### HEWL fibers help PD species disperse well in an aqueous solution

We generated HEWL fibers by treating HEWL with a high concentration of a strong denaturant (2 M of GdnHCl), which ensured rapid and reliable formation of amyloid fibers. The amyloid fibers that we synthesized had a morphology typically found in other amyloids (Figure 1A; ca. 8–13 nm thick and ca. 100–150 nm long),<sup>[17]</sup> forming an opaque and viscous solution that showed a peak of characteristic beta-sheet in a circular dichroism analysis (Figure S1).<sup>[18]</sup> The fibers were carefully quantified (described in the experimental section) and redispersed in a reaction mixture (pH 7.4, phosphate-buffered saline (PBS)) at

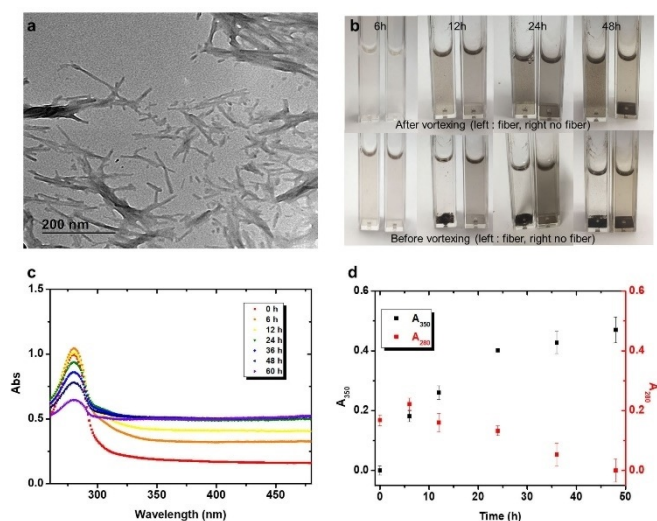


**Figure 1.** Influence of HEWL amyloid fibers on the formation of PD species. a) TEM image of HEWL amyloid fibers. b) Photos of solutions containing dopamine and HEWL fibers (left) and only dopamine (right) from 6 h to 48 h. Before measuring an absorption spectrum, each sample was redispersed by brief vortexing (top), in which the dispersion property was markedly altered by the presence of fibers. c) The absorbance spectrum of a reaction mixture (5  $\mu\text{M}$  of HEWL fibers and 250  $\mu\text{M}$  of dopamine) at different times. d) Changes in absorbance at specific wavelengths (280 nm for dopamine and 350 nm for PD species) over time.

the desired concentrations before incubating with various concentrations of dopamine under vigorous shaking (200 rpm). Compared to those without fibers, solutions of amyloid-dopamine mixtures turned dark faster, reflecting the accelerated formation of PD species. Figure 1B shows PD species formed under various conditions, which depicts another remarkable difference that amyloid fibers have caused; with fibers, large precipitates appeared within 12 h, and the precipitates were easily redispersed in the solution by a brief vortexing with the resulting suspension state remaining stable (i.e., not deposited on the bottom of the cuvette) for more than 30 min. Without fibers, on the other hand, such large floppy precipitates did not form until the late stage of the reaction, but once formed, they were very adhesive to the cuvette surface, making them hard to disperse in solution. Such differences indicate that PD species with HEWL fibers are preferentially adhesive to the fibers, whereas those without fibers assemble slowly into larger precipitates that tend to adhere to external surfaces, akin to what happens in PD coating.

To quantitatively examine the reaction progress, we measured the absorption spectra of the reaction mixture at different times. Figure 1C shows the formation of PD species in the solution, as evidenced by the gradual increase of the broad absorption in the UV/Vis region. We used optical density at the wavelength of 350 nm ( $A_{350}$ ) as a measure for the formation of PD species. The corresponding consumption of dopamine monomer, measured at 280 nm, was also observed over time (Figure 1D).

## HEWL fibers accelerate the formation of PD species

We next set out to ask whether HEWL fibers have an ability to accelerate the formation of PD species, by using four different concentrations of HEWL fibers (2.5, 5, 10, and 20  $\mu\text{M}$ ), while fixing the concentration of dopamine to 250  $\mu\text{M}$ . We assumed that a single molecule of HEWL would provide roughly 10–15 interacting sites for catechol, considering the numbers of side chains (e.g., 18 for cationic and 10 for aromatic, while assuming roughly half of them are sufficiently exposed) that possibly interact with catechols, and thus the selected sets of concentrations were intended to make the concentrations of the interacting pair comparable. Increasing the quantity of fibers did not alter the visual appearance of PD-fiber complexes or their susceptibility to vortexing; all the samples contained dark precipitates that could be dispersed by a brief vortexing. Higher concentration of fiber, however, led to the formation of darker solution, and higher light absorption across a broad range of wavelength (Figure S2 and Figure S3). Monitoring the value of  $A_{350}$  for each sample showed such a trend more clearly (Figure 2A), indicating that the fibers accelerated the formation of

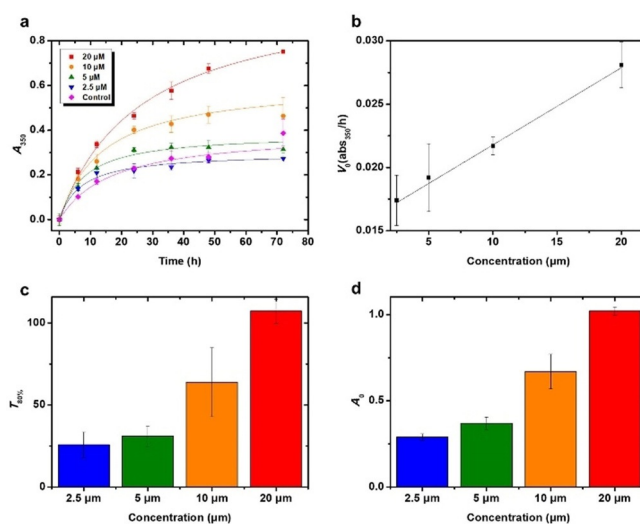


**Figure 2.** Kinetic analyses. a) Time-dependent changes of  $A_{350}$  values at four fiber concentrations (fixed dopamine concentration of 250  $\mu\text{M}$ ). b) Plot of the initial velocities of the formation of PD species (measured by using  $A_{350}$  values between 0 h and 12 h) versus the concentration of HEWL fibers. Plots of c)  $T_{80\%}$  and d)  $A_0$  values at each condition.

PD species in a quantitative manner. We could fit the time-dependent change of  $A_{350}$  values with different concentrations of fibers to a logistic time evolution function [Eq. (1)]:

$$A_{350}(t) = A_0 \left( 1 - \frac{1}{1 + \frac{t}{t_0}} \right) \quad (1)$$

in which  $A_0$  is the maximum absorption value, and  $t_0$  is the constant that determines how fast the reaction reaches a plateau (Figure 3A). Notably, this function is mathematically simi-

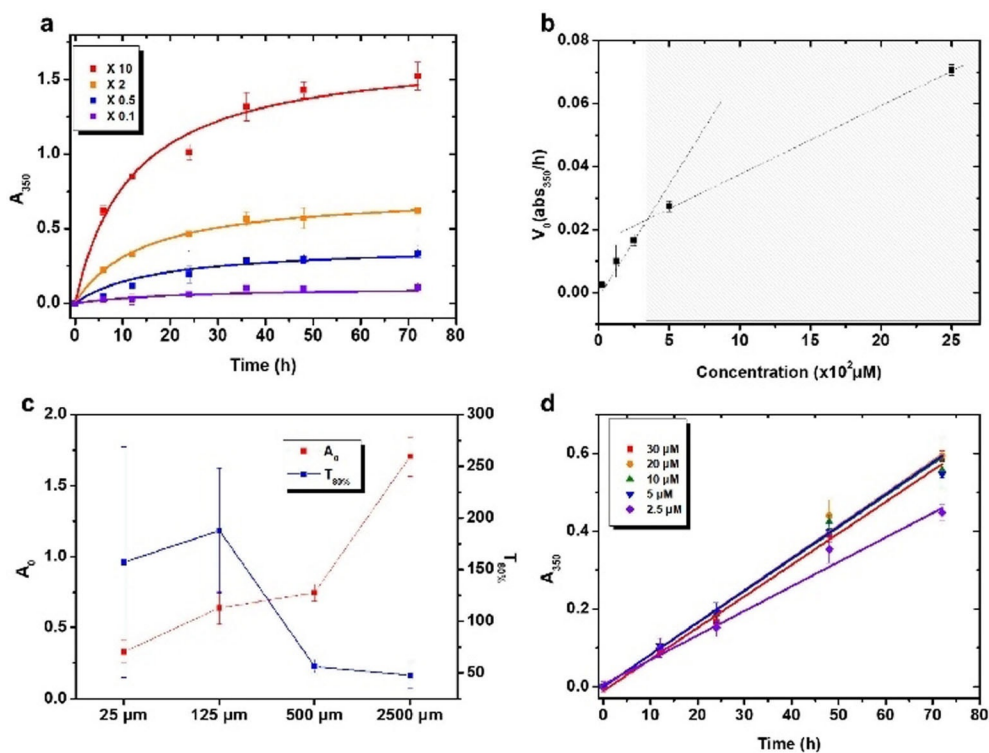


**Figure 3.** Kinetic analyses under dopamine-excess and monomer conditions. a) Time-dependent changes of  $A_{350}$  values at different dopamine concentrations (fixed HEWL fiber concentration of  $5 \mu\text{M}$ ). b) Plot of the initial velocities of the formation of PD species (measured by using  $A_{350}$  values between 0 h and 12 h) versus the concentration of dopamine. The graph can be roughly divided into two parts, each representing a distinct reaction process. c) A plot of  $A_0$  and  $T_{80\%}$  values for each condition. d) Time-dependent changes of  $A_{350}$  values at different concentrations of HEWL monomers (fixed dopamine concentration of  $250 \mu\text{M}$ ).

lar to the kinetic profile of product formation by a second-order homogeneous association, or heterogeneous one when the concentrations of the two reactants are similar. In each sample, the initial velocity of the reaction (measured between 0–12 h) was linearly proportional to the quantity of HEWL fibers provided, implying that the reaction determining step of the formation of PD-amyloid complex is approximately first-order to the fiber (Figure 2B). The time to reach a plateau ( $t_{80}$ ; which we parameterized as the time to reach an 80% value of  $A_0$ ), and  $A_0$  were also proportional to the quantity of fibers (Figure 2C and D). The results suggest, albeit indirectly, that the “reactive sites” at the surface of the fibers (or within them) are gradually blocked as the reaction progresses, making its rate progressively slower.

When the quantity of fibers was fixed to  $5 \mu\text{M}$  and the concentration of dopamine was greatly increased (from  $25 \mu\text{M}$  to  $2500 \mu\text{M}$ , which is in a dopamine-excess region), the kinetic profile of  $A_{350}$  values fit to the logistic function in a different fashion (Figure 3A and Figure S4). The initial velocity of the reaction in this case was again linearly proportional to the concentration of dopamine at the lower concentration region, but it deviated from the trend line at the excess condition (Figure 3B), indicating that the excess amount of dopamine brings about the onset of another pathway of forming PD species, which only relies on  $\text{O}_2$ -driven oxidation of dopamine, but is irrespective of HEWL fibers. In line with this, increasing the con-

centration of dopamine gave rise to the value of  $A_0$ , but led to an inconsistent trend in the value of  $t_{80}$  (Figure 3C). Based on these results, we could speculate that the presence of HEWL fibers leads to an accelerated pathway for the formation of PD species, in which the second-order heterogeneous association of a molecule of dopamine with a reactive site (or a functional group) of fibers play a primary role.

We note that 1) because of the insolubility and extreme molecular heterogeneity of PD species, we had to use an indirect way (light absorption) to quantify the total amount of product mixtures, and thus the obtained kinetic parameters gave collective, semi-quantitative information. 2) The lack of molecular-scale understanding of catechol-amyloid interactions meant that we assumed the effective concentration of reactive sites on the fibers was simply proportional to that of HEWL molecules. 3) Although we tried to optimize reaction conditions, there was always at least one side reaction:  $\text{O}_2$ -dependent auto-oxidation of dopamine, which would also cause weak, but dose-dependent gradual changes in  $A_{350}$  value (as shown by the results of dopamine-excess or dopamine-only reactions (Figure S5 and S6)). Nonetheless, the kinetic analyses presented above provided simplified but intuitive implications on how PD species are formed, especially at the surface of amyloid fibers.



### HEWL monomers do not influence the kinetics of PD species formation

To ask if the observed accelerative effect was the property of HEWL in general, we conducted the same reaction in the presence of a non-aggregated (i.e., soluble) form of HEWL. Figure 3D shows time-dependent changes of  $A_{350}$  value in the presence of different concentrations of HEWL. To our surprise, soluble HEWL did have favorable influences on the formation of PD species, but the kinetic profiles of their formation differed greatly from those obtained with HEWL fibers. In our conditions (5–30  $\mu\text{M}$  of HEWL, measured until 72 h), soluble HEWL exhibited a marginal influence on the initial velocity of the formation of PD species, which remained constant (ca.  $0.008 \text{ h}^{-1}$ ; a similar rate to that of the only-dopamine conditions), but kept the reaction from reaching a plateau until 72 h except for 2.5  $\mu\text{M}$  of HEWL. Polydopamine species formed with HEWL monomers were more adhesive to surface of the cuvette and hard to disperse in solution, exhibiting similar materials properties to those formed only with dopamine (Figure S7). The observed kinetic profiles and materials properties suggest that HEWL monomers have limited participation in the reaction determining step for the polydopamine formation, but rather provide more reaction sites distributed throughout the entire solution, as opposed to those confined on fiber surfaces, ultimately increasing the quantity of PD species finally formed.

### HEWL fibers and monomers lead to PD species with distinct physicochemical properties

To compare the PD species formed in the presence of HEWL monomers and fibers, we conducted infrared (IR) spectroscopy and transmission electron microscopy (TEM) studies. We first obtained IR spectra of HEWL monomers and HEWL assembled as amyloid fibers. As previously reported,<sup>[19]</sup> the HEWL samples showed different shapes in their amide I peaks (Figure 4A), and the deconvolution analysis indicated that HEWL fibers contained more beta-sheet component ( $1630 \text{ cm}^{-1}$ ,  $1678 \text{ cm}^{-1}$ ), whereas soluble HEWL contained more alpha-helix and random coil component ( $1661 \text{ cm}^{-1}$ ,  $1645 \text{ cm}^{-1}$ ; Table S1). In

the same region, PD (i.e., those formed without HEWL) showed a monotonic decrease in peak intensity (Figure 4A), consistent with previous results.<sup>[20]</sup> Interestingly, IR spectra for PD species in the presence of soluble HEWL and HEWL fibers were similar to the summation of the peaks of PD and the corresponding original HEWL species, respectively (Figure 4A), indicating that the chemical structures of amides were unchanged after the formation of PD-HEWL composites. This means that the catechol-amyloid interaction and the subsequent formation of PD species did not remodel or disassemble amyloid fibers, but simply made them invisible to ThT analysis by physically encapsulating them. TEM analyses further supported the conclusion. Figure 4B shows TEM images of PD species formed with HEWL fibers. Notably, we could clearly observe the formation of bundled superhelical fibers coated with melanin species. The HEWL amyloid fibers had thickness of 15 nm, but after PD formation, the thickness of bundled fibers were 100–200 nm with helical morphology. Such bundled fibers were not observable in the only-dopamine species or those formed with soluble HEWL, which both showed mesh-like structures (Figure 4C). This result suggests that the PD species played roles in bundling the preformed amyloid fibers and forming compact composite materials, rather than disassembling or remodeling them. It is possible that PD species have interfered with optical analyses conducted in previous works, and thus made amyloid fibers seem disassembled.

### Pmel17 fibers are functionally similar to HEWL fibers

Finally, we set out to compare the capability of amyloid fibers of recombinant Pmel17 and its subdomains in facilitating the formation of PD species to that of HEWL fibers. We chose NTD, PKD, and the full domain of Pmel17, according to the previous report, which compared the fibril-forming properties of each subdomain (Figure 5A).<sup>[5a]</sup> As previously reported, all domains of Pmel17 instantaneously formed fibers when they were diluted from a high concentration of a denaturant (six-fold dilution of an 8 M urea-containing solution to that without). White precipitates appeared immediately upon dilution, and each sample exhibited high ThT fluorescence intensity (Figure S9).

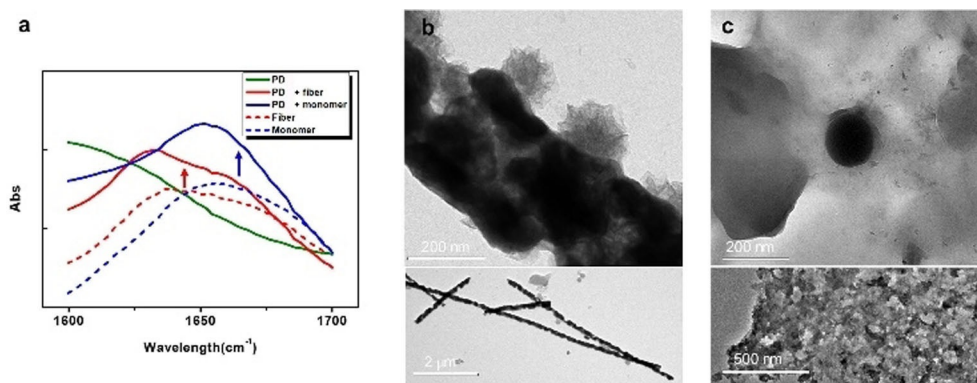


**Figure 4.** Characterization of PD species. a) FTIR spectra of HEWL monomer and fiber, PD species, and PD species synthesized in the presence of HEWL monomer and fiber. TEM images of melanin-like species containing b) HEWL fibers and c) HEWL monomers. High-resolution (upper) and low-resolution (lower) images.

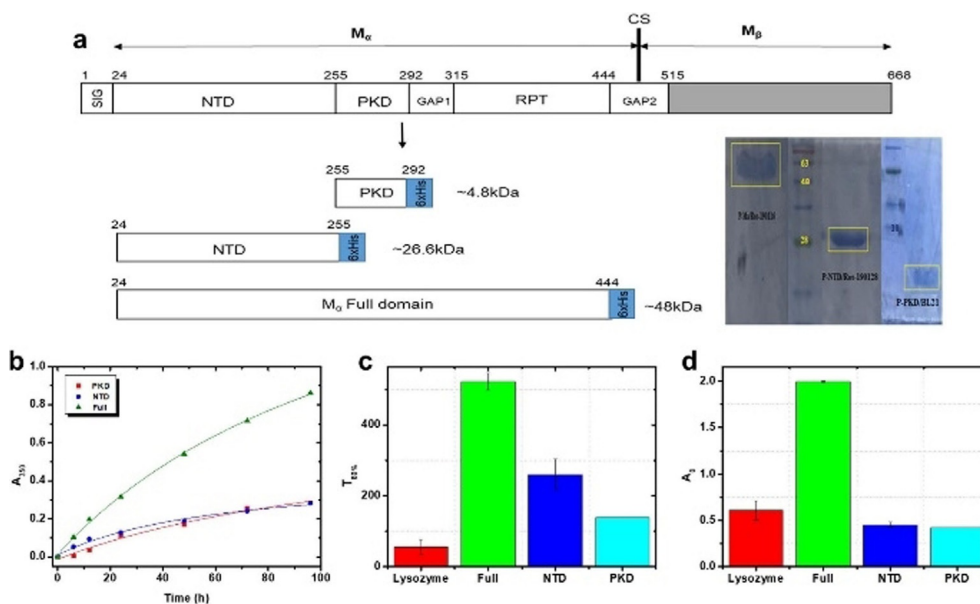


**Figure 5.** PD species formed in the presence of Pmel17 proteins. a) Gene maps of Pmel17 and its subdomains and the whole-cell gel images of NTD, PKD, and M $\alpha$  full domain. b) Time-dependent changes of  $A_{350}$  values in samples containing fibers made of each protein at 10  $\mu\text{M}$  (fixed dopamine concentration of 250  $\mu\text{M}$ ). Plots of c)  $T_{80\%}$  and d)  $A_0$  values under each set of conditions.

The materials properties of each fiber (e.g., dispersion in solution, elasticity, and turbidity) were, however, very different from the others. The fibers were quantified (10  $\mu\text{M}$ ) in the same way with HEWL, and incubated with dopamine (250  $\mu\text{M}$ ). The kinetic profiles in the presence of each fiber also fit to the same logistic function (Figure 5B). Compared to the same mass equivalent of HEWL fibers, the amyloid fibers of the full domain Pmel17 showed higher  $t_{80}$  and  $A_0$  values, indicating that they provide more sites reactive for synthesizing PD species, but the actual rate of the reaction was comparable (measured to be 0.0124  $\text{h}^{-1}$ ). Its subdomains, on the other hand, were observed to be less efficient both in accelerating the reaction and providing more reactive sites (Figure 5C and D). The differences between full-domain Pmel17 and its subdomains likely stem from their different aggregating tendencies; ThT fluorescence intensity gives information on the presence of cross- $\beta$ -sheet components, and is often inadequate as a metric for evaluating the maturation of the amyloid structure. Questions regarding which sub-domain plays a role as a core-component of Pmel17 and what is the exact role of each sub-domain, merit further examinations, but it is likely that the full domain is required to assemble matured amyloid fibers (there are many possible structures insoluble and active for ThT fluorescence, but of a low content of matured amyloids).

## Conclusion

The results presented above provide the following implications on the roles of amyloid fibers in the process of PD formation (Figure 6): 1) a biologically irrelevant protein, to a different extent for different proteins, can actively participate in the formation of PD species. Addition of molecules of a protein results in more PD species under the same reaction condition

(e.g., pH, temperature, and dopamine quantity). This can be connected to a recent result of Lee et al., who showed that the formation of dopamine-melanin pigment is mainly driven by cation- $\pi$  progressive assembly, in which cationic molecules play central roles.<sup>[21]</sup> Proteins have cationic side chains, such as amine and arginine, which can act as “active sites” for inducing the formation of PD species, yet they can also be covalently crosslinked with quinone groups, leaving multiple interacting pathways feasible.<sup>[9c]</sup> 2) Matured amyloid fibers can not only provide reactive sites but can also accelerate the formation of PD species. Here, the reactive sites are confined to the surface of the fibers and are gradually covered by PD species during the reaction, while, thanks to their adhesive character, bundling the fibers into thicker helical structures. The association of dopamine or one of its oxidized forms with an active site on the fibers is likely the rate-determining step in the accelerated pathway of melanogenesis. 3) Bundling of fibers has two major ramifications. Bundling, which becomes more notably as the reaction progresses, would increase the local concentration of relevant reactants, possibly further accelerating the reaction, although it is not diffusion-limited. This, in turn, adds an autocatalytic character to the reaction kinetics, as we experimentally showed in the logistic formation profile. In addition, bundled form of PD-fiber composites have greatly different materials properties from those formed without fibers. Those with fibers are better dispersed in aqueous environments than those without, preventing themselves from sticking to external surfaces. 4) It is uncertain whether the chemical driving forces responsible for attractive amyloid fiber-dopamine interactions are general for all pairs of proteins and catechols, or each case has a distinct chemistry. For example, Kelly et al. suggested hydrophobic association between an aromatic system of dopamine and a cross- $\beta$ -sheet structure in amyloids is a major driving

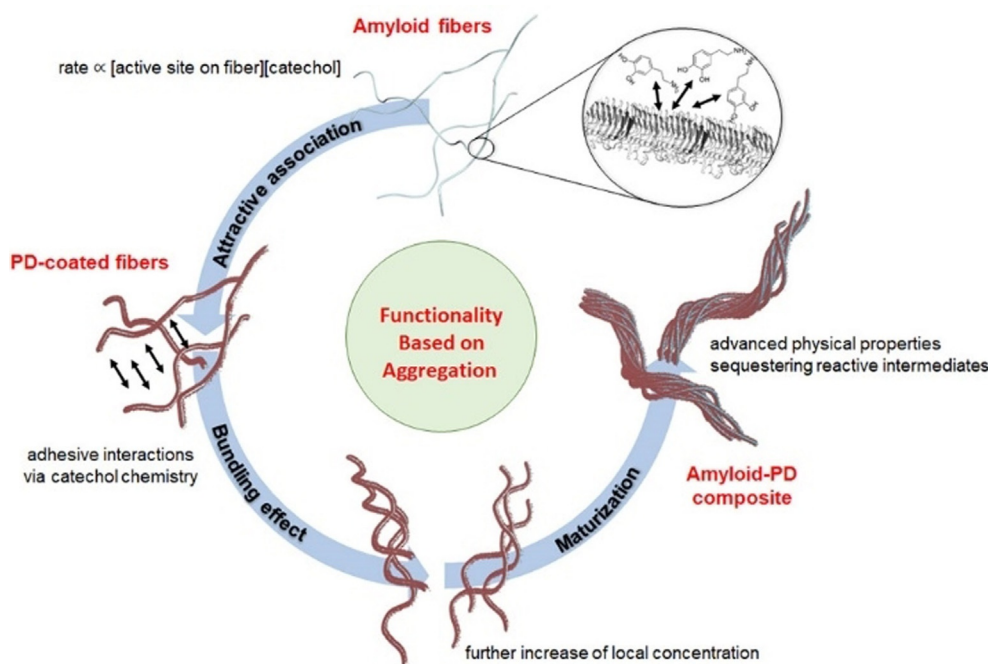


Figure 6. Suggested roles of amyloid fibers in melanin biosynthesis.

force for remodeling amyloid fibers by EGCG.<sup>[22]</sup> Although complete disassembly or drastic remodeling of fibrillar structures were absent in the current work, such hydrophobic interaction cannot be ruled out when describing the attractive relationship of amyloid and dopamine.

Melanin is chemically heterogeneous and relatively poorly defined, yet recent reports are starting to reveal that properties and functions of various melanins (e.g., solubility, radical properties, light absorption, and film-forming properties) can be dramatically altered depending on polymerization conditions or chemical components.<sup>[23]</sup> In one example, Ulijn et al. showed that properties of melanin-like pigments can be tuned by controlling supramolecular order of catechols (by means of peptide aggregation) before their oxidation.<sup>[24]</sup> The results of this work imply that Pmel17 fibers may be a sophisticated scaffold, rather than a simple physical matrix material. We showed that a protein that is irrelevant to melanogenesis can regulate oxidative polymerization of dopamine in a similar manner to melanin biosynthesis. Remarkably, it fulfills such regulatory roles only when aggregated into amyloid fibers, likely relying on a combination of multiple noncovalent (or covalent but reversible) interactions. The current work thus implies that the amyloid quaternary structures *per se* may facilitate the formation of melanin (both in quantity and rate), sequester toxic intermediates, and tune the material properties of the final form. We have used HEWL, which is very different from Pmel17 in many aspects (including isoelectric point, size, and polarity), and they thus have different aggregation pathways. When they form matured amyloid fibers, however, both of them, and fibers of other proteins as well, periodically present a set of side chains at their surfaces by means of  $\beta$ -sheet assembly, which makes the results obtained with HEWL fibers

valid for studying the role of Pmel17 fibers, or functional amyloids in general. Collectively, we suggest that amyloid aggregation is one of nature's ways to control molecular order/concentration at a large surface. Such a method of designing chemical functionality relies on transient, nonspecific, and weak multivalent interactions, which are frequently utilized in nature (as shown in recent studies of membrane-less organelles), but less so in artificial systems.

## Acknowledgements

This work was supported by the National Research Foundation of Korea (NRF) grant funded by the Ministry of Science, ICT & Future Planning (MSIP) (2019R1C1C1009111), and the GRR program of Gyeonggi province [GRR-kyunghee2017(A01)].

## Conflict of interest

The authors declare no conflict of interest.

**Keywords:** amyloid beta-peptides · bioorganic chemistry · melanin biosynthesis · peptides · polydopamine

- [1] a) Y. L. Liu, K. L. Ai, L. H. Lu, *Chem. Rev.* **2014**, *114*, 5057–5115; b) H. Lee, S. M. Dellatore, W. M. Miller, P. B. Messersmith, *Science* **2007**, *318*, 426–430; c) B. P. Lee, P. B. Messersmith, J. N. Israelachvili, J. H. Waite, *Annu. Rev. Mater. Res.* **2011**, *41*, 99–132.
- [2] a) D. R. Dreyer, D. J. Miller, B. D. Freeman, D. R. Paul, C. W. Bielawski, *Langmuir* **2012**, *28*, 6428–6435; b) J. H. Ryu, P. B. Messersmith, H. Lee, *ACS Appl. Mater. Interfaces* **2018**, *10*, 7523–7540.
- [3] M. d'Ischia, A. Napolitano, V. Ball, C. T. Chen, M. J. Buehler, *Acc. Chem. Res.* **2014**, *47*, 3541–3550.

- [4] D. M. Fowler, A. V. Koulov, C. Alory-Jost, M. S. Marks, W. E. Balch, J. W. Kelly, *PLoS Biol.* **2006**, *4*, 100–107.
- [5] a) R. P. McGlinchey, F. Shewmaker, P. McPhie, B. Monteroso, K. Thurber, R. B. Wickner, *Proc. Natl. Acad. Sci. USA* **2009**, *106*, 13731–13736; b) B. Watt, G. van Niel, D. M. Fowler, I. Hurbain, K. C. Luk, S. E. Stayrook, M. A. Lemmon, G. Raposo, J. Shorter, J. W. Kelly, M. S. Marks, *J. Biol. Chem.* **2009**, *284*, 35543–35555; c) R. P. McGlinchey, J. M. Gruschus, A. Nagy, J. C. Lee, *Biochemistry* **2011**, *50*, 10567–10569; d) R. P. McGlinchey, F. Shewmaker, K. N. Hu, P. McPhie, R. Tycko, R. B. Wickner, *J. Biol. Chem.* **2011**, *286*, 8385–8393; e) B. Watt, G. van Niel, G. Raposo, M. S. Marks, *Pigm. Cell Melanoma. R.* **2013**, *26*, 300–315.
- [6] T. H. Vu, T. Shimanouchi, N. Shimauchi, H. Yagi, H. Umakoshi, Y. Goto, R. Kuboi, *J. Biosci. Bioeng.* **2010**, *109*, 629–634.
- [7] a) J. Li, M. Zhu, A. B. Manning-Bog, D. A. Di Monte, A. L. Fink, *FASEB J.* **2004**, *18*, 962–964; b) F. Orsini, D. Ami, A. Lascialfari, A. Natalello, *Int. J. Biol. Macromol.* **2018**, *111*, 1100–1105; c) S. Nusrat, N. Zaidi, M. K. Siddiqi, M. Zaman, I. A. Siddique, M. R. Ajmal, A. S. Abdelhameed, R. H. Khan, *Int. J. Biol. Macromol.* **2017**, *99*, 630–640.
- [8] a) J. Bieschke, J. Russ, R. P. Friedrich, D. E. Ehrnhoefer, H. Wobst, K. Neugebauer, E. E. Wanker, *Proc. Natl. Acad. Sci. USA* **2010**, *107*, 7710–7715; b) D. E. Ehrnhoefer, J. Bieschke, A. Boeddrich, M. Herbst, L. Masino, R. Lurz, S. Engemann, A. Pastore, E. E. Wanker, *Nat. Struct. Mol. Biol.* **2008**, *15*, 558–566.
- [9] a) M. Hirohata, K. Hasegawa, S. Tsutsumi-Yasuhara, Y. Ohashi, T. Ookoshi, K. Ono, M. Yamada, H. Naiki, *Biochemistry* **2007**, *46*, 1888–1899; b) H. J. Heo, D. O. Kim, S. J. Choi, D. H. Shin, C. Y. Lee, *J. Agric. Food Chem.* **2004**, *52*, 4128–4132; c) M. Sato, K. Murakami, M. Uno, Y. Nakagawa, S. Katayama, K. Akagi, Y. Masuda, K. Takegoshi, K. Irie, *J. Biol. Chem.* **2013**, *288*, 23212–23224.
- [10] K. A. Conway, J. C. Rochet, R. M. Bieganski, P. T. Lansbury, *Science* **2001**, *294*, 1346–1349.
- [11] S. Sieste, T. Mack, C. V. Synatschke, C. Schilling, C. M. Zu Reckendorf, L. Pendi, S. Harvey, F. S. Ruggieri, T. P. J. Knowles, C. Meier, D. Y. W. Ng, T. Weil, B. Knoll, *Adv. Healthcare Mater.* **2018**, *7*, 1701485.
- [12] M. Bisaglia, L. Tosatto, F. Munari, I. Tessari, P. P. de Laureto, S. Mammi, L. Bubacco, *Biochem. Biophys. Res. Commun.* **2010**, *394*, 424–428.
- [13] H. T. Li, D. H. Lin, X. Y. Luo, F. Zhang, L. N. Ji, H. N. Du, G. Q. Song, J. Hu, J. W. Zhou, H. Y. Hu, *FEBS J.* **2005**, *272*, 3661–3672.
- [14] F. Chiti, C. M. Dobson, *Nat. Chem. Biol.* **2009**, *5*, 15–22.
- [15] a) A. E. Cao, D. Y. Hu, L. H. Lai, *Protein Sci.* **2004**, *13*, 319–324; b) N. Yagi, N. Ohta, T. Matsuo, *Int. J. Biol. Macromol.* **2009**, *45*, 86–90; c) L. N. Arnaudov, R. de Vries, *Biophys. J.* **2005**, *88*, 515–526; d) S. Y. Ow, D. E. Dunstan, *Soft Matter* **2013**, *9*, 9692–9701.
- [16] B. A. Vernaglia, J. Huang, E. D. Clark, *Biomacromolecules* **2004**, *5*, 1362–1370.
- [17] a) M. Saiki, K. Shiba, M. Okumura, *FEBS Lett.* **2015**, *589*, 3541–3547; b) W. F. Xue, A. L. Hellewell, E. W. Hewitt, S. E. Radford, *Prion* **2010**, *4*, 20–25.
- [18] a) N. J. Greenfield, *Nat. Protoc.* **2006**, *1*, 2876–2890; b) Y. Wei, A. A. Thyparambil, R. A. Latour, *BBA-Proteins Proteom.* **2014**, *1844*, 2331–2337.
- [19] a) W. Dzwolak, V. Smirnovas, R. Jansen, R. Winter, *Protein Sci.* **2004**, *13*, 1927–1932; b) H. Hiramatsu, T. Kitagawa, *BBA-Proteins Proteom.* **2005**, *1753*, 100–107.
- [20] a) H. Coskun, A. Aljabour, L. Uiberlacker, M. Strobel, S. Hild, C. Cobet, D. Farka, P. Stadler, N. S. Sariciftci, *Thin Solid Films* **2018**, *645*, 320–325; b) F. B. Luo, K. Wu, J. Shi, X. X. Du, X. Y. Li, L. Yang, M. G. Lu, *J. Mater. Chem. A* **2017**, *5*, 18542–18550.
- [21] S. Hong, Y. Wang, S. Y. Park, H. Lee, *Sci. Adv.* **2018**, *4*, eaat7457.
- [22] F. L. Palhano, J. Lee, N. P. Grimster, J. W. Kelly, *J. Am. Chem. Soc.* **2013**, *135*, 7503–7510.
- [23] a) M. Ambrico, P. F. Ambrico, A. Cardone, N. F. Della Vecchia, T. Ligonzo, S. R. Cicco, M. M. Talamo, A. Napolitano, V. Augelli, G. M. Farinola, M. d'Ischia, *J. Mater. Chem. C* **2013**, *1*, 1018–1028; b) S. Ito, N. Suzuki, S. Takebayashi, S. Commo, K. Wakamatsu, *Pigm. Cell Melanoma. R.* **2013**, *26*, 817–825; c) L. Panzella, G. Gentile, G. D'Errico, N. F. Della Vecchia, M. E. Errico, A. Napolitano, C. Carfagna, M. d'Ischia, *Angew. Chem. Int. Ed.* **2013**, *52*, 12684–12687; *Angew. Chem.* **2013**, *125*, 12916–12919; d) A. Corani, A. Huijser, T. Gustavsson, D. Markovits, P. A. Malmqvist, A. Pezzella, M. d'Ischia, V. Sundstrom, *J. Am. Chem. Soc.* **2014**, *136*, 11626–11635.
- [24] A. Lampel, S. A. McPhee, H. A. Park, G. G. Scott, S. Humagain, D. R. Hekstra, B. Yoo, P. W. J. M. Frederix, T. D. Li, R. R. Abzalimov, S. G. Greenbaum, T. Tuttle, C. H. Hu, C. J. Bettinger, R. V. Uljijn, *Science* **2017**, *356*, 1064–1068.

---

Manuscript received: January 24, 2020

Revised manuscript received: February 19, 2020

Accepted manuscript online: February 24, 2020

Version of record online: April 15, 2020